Progress In Electromagnetics Research B, Vol. 55, 131–149, 2013

AN INTRODUCTION TO A MEDIUM FREQUENCY PROPAGATION CHARACTERISTIC MEASUREMENT METHOD OF A TRANSMISSION LINE IN UNDERGROUND COAL MINES

Jingcheng Li*, Joseph A. Waynert, and Bruce G. Whisner

National Institute for Occupational Safety and Health, 626 Cochran's Mill Road, Pittsburgh, PA 15236, USA

Abstract—An underground coal mine medium frequency (MF) communication system generally couples its electromagnetic signals to a long conductor in a tunnel, which acts as a transmission line, and exchanges signals with transceivers along the line. The propagation characteristics of the transmission line, which is usually the longest signal path for an MF communication system, play a major role in determining the system performance. To measure the MF propagation characteristics of transmission lines in coal mine tunnels, a method was developed based on a basic transmission line model. The method will be presented in this paper along with the propagation measurements on a transmission line system in a coal mine using the method. The measurements confirmed a low MF signal power loss rate, and showed the influence of the electrical properties of surrounding coal and rock on the MF propagation characteristics of the line.

1. INTRODUCTION

In this paper, we present a method of obtaining the medium frequency (MF) (300 kHz–3 MHz) propagation characteristics of a transmission line (TL) system which is often used as a signal path for an MF communications system in a coal mine tunnel. The TL propagation parameters yielded from the method are: characteristic impedance, propagation attenuation constant, propagation phase constant, power loss rate, and velocity factor (a ratio of the signal velocity to the velocity of light in a vacuum). The method will be presented in this paper along with the propagation parameters obtained on a

Received 30 July 2013, Accepted 18 September 2013, Scheduled 25 September 2013

* Corresponding author: Jingcheng Li (Jingcheng.li@cdc.hhs.gov).

transmission line system in a coal mine tunnel. The propagation characteristics obtained confirmed the low MF signal loss on the transmission line. We also noticed the influence of the electrical properties of the surrounding coal and rock of the tunnel on the signal propagation characteristics.

1.1. MF Communication System

MF communication systems are attractive to the mining industry because of their relatively low cost, reduced infrastructure, and anticipated high reliability in operation compared to other mine communication systems. MF signals can propagate by electromagnetically coupling to an existing conductor such as an AC power cable, trolley wire, or a rail track commonly found in coal mine tunnels. The conductor serves as a parasitic signal path, and can support communications among low-power transceivers that may be many kilometers apart. The conductor is generally the longest signal path. Its signal propagation characteristics, hence, have a major influence on the performance of the communication system.

1.2. Study of Propagation Characteristics of Tunnel Transmission Line

Decades ago, it was found that a long conductor within a coal tunnel permitted an MF signal to propagate parasitically and travel great distances. Researchers have been attempting to characterize this phenomenon and build a mine MF communication system that can use the existing long metal infrastructure as its signal path [1–3].

A long conductor carrying RF signals running in a tunnel has been modeled as an RF TL in previous studies [1–7]. Consideration of a long conductor parallel to the ground surface to carry RF signals using a ground return was also modeled as an RF TL [8–11]. These studies indicated that propagation characteristics of an aboveground transmission line could be evaluated by taking the electrical properties (permittivity, permeability and conductivity) of the ground into account, suggesting that the propagation characteristics of a TL in a coal mine could also be estimated by taking the electrical properties of the surrounding coal and rock of the tunnel into account [6, 7].

The MF current measurements made on TLs in coal mines in the 1980s confirmed the low attenuation rate [2, 4, 5]. Measurements of the other TL propagation parameters needed for general MF propagation analysis are, however, seldom found in the published literature. One explanation for the lack of MF propagation data may be the absence of an effective measurement method.

We recently presented an easy-to-use method to obtain the characteristic impedance and power loss rate of a TL in a tunnel in [6, 7]. The method was developed based on a coaxial cable TL model for a longitudinal conductor in a tunnel. A coaxial cable has its center conductor carrying a forward signal and the outer conductor carrying the return signal. A tunnel TL can act as an enlarged coaxial cable with a conductor carrying a forward signal and the surrounding coal and rock the return signal. We expand on the previously reported method using the same coaxial model to obtain additional propagation parameters: the attenuation constant, phase constant and velocity factor in this paper.

2. TRANSMISSION LINE PROPAGATION PARAMETERS

Conductors in a mine tunnel are frequently hung from the roof as illustrated in Figures 1 and 2. The tunnel's TL equivalent circuit is shown in Figure 3. We use the transverse electromagnetic (TEM) approximation to estimate the propagation parameters [6, 7]. In Figure 3, $R(f)$ and $L(f)$ represent the equivalent series per-unit-length resistance and inductance of the conductor, coal, and rock, while $G(f)$ and $C(f)$ represent the per-unit-length shunt admittance and capacitance between the conducting materials.

It is known that the propagation characteristics of the TL in Figure 3 can be completely defined by two parameters: the characteristic impedance, $Z_0(f)$, and propagation constant, $\gamma(f)$, at a frequency f. Many references including [11–14] have provided the methods to determine the values of both $Z_0(f)$ and $\gamma(f)$ with the known values of $R(f)$, $L(f)$, $G(f)$, and $C(f)$. The voltage and current

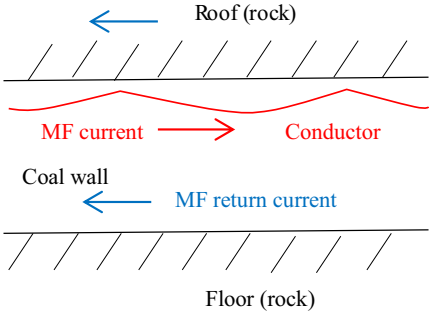

Figure 1. Conductor hung from roof in a tunnel.

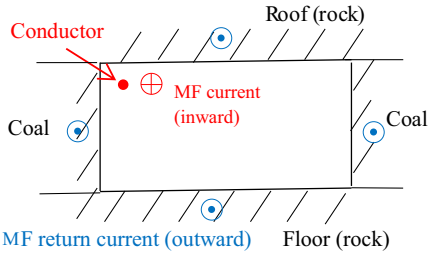

Figure 2. Cross section of tunnel with a conductor.

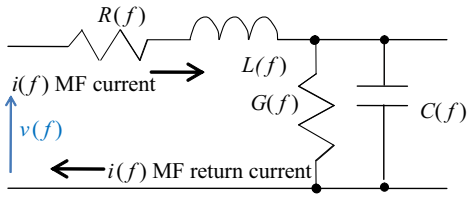

Figure 3. Equivalent circuit of a tunnel TL.

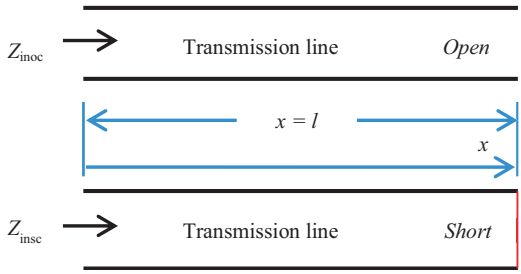

Figure 4. Input open and shorted line impedances of TL of length of l.

propagating along the TL can then be characterized with (1) and (2), where $V(f, x)$ and $I(f, x)$ are the voltage and current at a point along the line at a distance x from the incident voltage source. As shown in (3), $\gamma(f)$ has two components, $\alpha(f)$, the real part of $\gamma(f)$, denoting the attenuation constant, and $\beta(f)$, the imaginary part, the phase constant. With known values of $R(f)$, $L(f)$, $G(f)$, and $C(f)$, the values of $\gamma(f)$ and $Z_0(f)$ of a TL can be determined using (A5) and (A8) in the Appendix. However, it is difficult to make the measurements of $R(f)$, $L(f)$, $G(f)$, and $C(f)$ in a coal mine environment.

Previous research [13] showed that a pair of open and shorted line impedance measurements at a given frequency at the input end of the TL could be used to derive the characteristic impedance, $Z_0(f)$, the power loss rate, $Loss(f)$, and the propagation attenuation constant, $\alpha(f)$, as given in (4), (5), and (6). Figure 4 illustrates the configuration for the measurements of an open line impedance, $Z_{\text{inoc}}(f)$, and a shorted line impedance, $Z_{\text{insc}}(f)$, at the input end of a TL of length $x = l$. Also as shown in previous research [13], multiple pairs of $Z_{\text{inoc}}(f)$s and $Z_{\text{insc}}(f)$s at different frequencies can be used to obtain $\beta(f)$ from (7), the propagation velocity, $v_{\text{p}}(f)$, from (8), and velocity factor, $VF(f)$, from (9). (The Appendix describes the input phase

$2\beta(f)l$ used in (7)). In (9), the velocity of 3.0×10^8 m/s for light is used to obtain a velocity factor. (Power loss rate and velocity factor are usually given by manufacturers as part of TL specifications.) We take this same approach in the development of the method.

$$V(f,x) = V_0^+ e^{-\gamma(f)x} + V_0^- e^{\gamma(f)x} \tag{1}$$

$$I(f,x) = (1/Z_0(f)) \left(V_0^+ e^{-\gamma(f)x} - V_0^- e^{\gamma(f)x} \right) \tag{2}$$

at a distance of x from incident source V_0^+, V_0^-: reflected voltage

$$\gamma(f) = \alpha(f) + j\beta(f) \tag{3}$$

$$Z_0(f) = \sqrt{Z_{\text{insc}}(f) \cdot Z_{\text{inoc}}(f)} \text{ (Ohms)} \tag{4}$$

$$Loss(f) = \frac{8.686}{2l} \left| \frac{1+\sqrt{Z_{\text{insc}}(f)/Z_{\text{inoc}}(f)}}{1-\sqrt{Z_{\text{insc}}(f)/Z_{\text{inoc}}(f)}} \right| \left(\frac{\text{dB}}{\text{Unit length}} \right) \tag{5}$$

$$\alpha(f) = \frac{1}{2l} \left| \frac{1+\sqrt{Z_{\text{insc}}(f)/Z_{\text{inoc}}(f)}}{1-\sqrt{Z_{\text{insc}}(f)/Z_{\text{inoc}}(f)}} \right| \left(\frac{\text{Nepers}}{\text{Unit length}} \right) \tag{6}$$

$$\beta\left(f = \frac{f_2+f_1}{2} \right) = \frac{\pi(f_2+f_1)}{2l(f_2-f_1)} \left(\frac{\text{Rad}}{\text{Unit length}} \right) \tag{7}$$

for $f_2 > f_1$, where frequencies f_2 and f_1 are selected to make $2\beta(f)l$ have a difference of 2π.

$$v_p\left(f = \frac{f_2+f_1}{2} \right) = \frac{\pi(f_2+f_1)}{\beta} \left(\frac{\text{meters}}{s} \right) \tag{8}$$

$$VF(f) = \frac{v_p(f)}{3.0 \times 10^8} \tag{9}$$

3. METHOD FOR TUNNEL TRANSMISSION LINE

Our TL characterization method requires an impedance measurement system to acquire open and shorted line impedances on a tunnel TL. We found that there were three major considerations in the development of such a measurement system. The first was the selection of an impedance measurement device. The second was to find a way to collect return current from the coal and rock in the tunnel in order to obtain reliable impedance measurements. The third was to reduce RF interference of electromagnetic noise conducted in the coal and rock. An LCR meter (Agilent E4980A) was shown to be a reliable and repeatable impedance measurement device in [6, 7], and the techniques introduced in [6, 7] also proved effective to resolve the issues of the current collection and ground RF interference.

The method requires construction of the grounding interfaces at both ends of the TL to collect return current flowing through the solid coal and rock strata for impedance measurements on the TL. In this study, a number of stainless steel bolts were tightly screwed into the coal and rock around the tunnel surface perimeter forming an electrical interface. The impedance of the TL return path formed with the coal and rock strata could then be automatically accounted for in the line's open and short circuit impedance measurements. Our experimental data showed that six bolts or more are generally needed at each end of the TL to obtain relatively accurate open and shorted line impedance measurements.

In our initial attempt to measure TL impedances, we discovered significant RF noise conducted in the coal and rock. The high power components of the noise were usually below 50 kHz. The received power of DC, 60 Hz and its harmonics could often saturate the impedance measurement device if not filtered out. A 0.01-μF capacitor in series with the LCR lead proved to be effective at blocking these noise components [6, 7] and were used in this study.

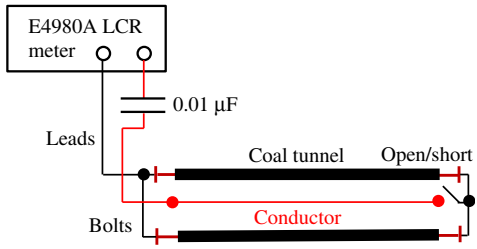

Figure 5. Measurement system for a TL system in a mine tunnel.

The complete measurement system is illustrated in Figure 5, where an Agilent E4980A LCR meter is used as an impedance measurement device. The bolts are inserted in the coal and rock around the tunnel surface perimeter forming the electrical interfaces at both ends of the conductor. A 0.01-μF capacitor serves as a high-pass filter to attenuate the low frequency noise components. The lead wires were needed to make a connection of the conductor and the coal and rock interface to the LCR meter. The lead wires and the capacitor would inevitably introduce additional impedances to the impedance measurements on the TL, and the technique given in [6, 7] was used to remove their effect from the LCR meter readings. The lead wires were kept as short as possible to minimize their impact on the impedance measurements.

To efficiently collect and process a large quantity of measurements

and ensure data integrity, several pieces of software were also developed in the study of the method. They included (1) LabVIEW-based data acquisition software to control the LCR meter and automatically collect measurements from the TL, (2) C++-based and Excel-based data pre-processing software to remove the lead and capacitor impedance from the readings of the LCR meter to obtain line's true impedance measurements, and (3) the software to compute the line's propagation parameters.

Three sets of the independent impedance measurements as a function of frequency were acquired on the TL in the data acquisition stage. The measurements were performed in a relatively short time so that variations in temperature and humidity, for example, would not affect the readings. The measurements included one set of the lead impedance measurements with the capacitor included, and two sets of the line impedance measurements — one for the open and one for the short. The lead impedances were removed from both the open and shorted line impedance measurements, and the results were then used to derive the propagation parameters for the TL in the data processing stage.

4. PROPAGATION CHARACTERISTICS OF A TUNNEL TRANSMISSION LINE SYSTEM

The method was applied to an existing 562-m-long twisted pair mine telephone cable hung in a tunnel in the Safety Research Coal Mine (SRCM) in Pittsburgh, Pennsylvania, for a test. The diameter of each copper core wire of the cable was 1.40 mm with a radial plastic insulation thickness of about 1.0 mm. The cable was configured as a single-conductor line by shorting the two wires together at each end

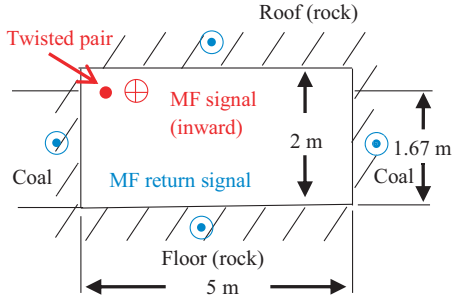

Figure 6. Tunnel cross-sectional dimensions and conductor location in the SRCM.

of the cable. The SRCM is a room and pillar mine with the average tunnel cross-sectional dimensions and the cable position in the tunnel as shown in Figure 6. Because of the periodic sag of the cable and uneven coal wall, the distance between the cable and the rock roof or the coal wall varied from several to about 20 cm. The electrical connection to the tunnel walls was through 6 bolts 7.9 mm in diameter and 152.4 mm long which were screwed into the tunnel coal and rock at each end of the cable. The distance between any two bolts at either end varied from 0.40 m and 0.61 m depending on the available area of the coal and rock surfaces. An area with no visible cracks in the solid coal and rock body was selected for the bolt locations.

Over 1,700 pairs of the open and shorted line impedance measurements of the cable together with over 1,700 of the corresponding lead impedance measurements were first acquired at frequencies from 300 kHz to 2 MHz, mostly in a step of 1 kHz. The characteristic parameters were then derived from the measurements. The parameters are presented next mostly in plots to accommodate the large amount of data.

4.1. Coal and Rock Impedance

One of the major differences between a coaxial cable and a tunnel TL system is the materials of their outer conducting layers. The outer layer for a coaxial cable is metal, but for the tunnel TL system the outer layer is the thick coal and rock strata. The test offered an opportunity to investigate the influence of the coal and rock on the propagation characteristics of the TL system. For the grounding system at each end of the TL, we measured the impedances between every two bolts and every two groups of bolts at the electrical interfaces with the LCR meter. These impedances give some information on the electrical properties of coal and rock in the MF band. Figure 7 shows a representative sample of the many sets of the measurements we took between two groups of bolts in coal and rock. The measured resistance and reactance had a frequency response similar to the impedance. The coal and rock impedances are clearly non-linearly dependent on frequency. The measurements also showed that the impedances between different groups of bolts were different. Figure 7 shows an example of the highest impedance readings among all of the possible groupings of bolts.

4.2. Open and Shorted Line Impedances

The open and shorted line impedances of the twisted cable acting as a single-conductor TL system with the corresponding impedances of

the leads removed are given in Figure 8. The periodic peaks and valleys of both the open and shorted line impedances are the result of the frequency variation of the voltage and current standing waves as measured at the input end of the line.

4.3. Characteristic Impedance

The characteristic impedance, $Z_0(f)$, of the single-conductor twisted cable TL system is derived from (4). Figure 9 shows the plot of the characteristic impedance as a function of frequency. The behavior of the characteristic impedance is reminiscent of the coal and rock impedance distribution shown in Figure 7, indicating the influence of the electrical properties of the coal and rock on the characteristic impedance of the TL system.

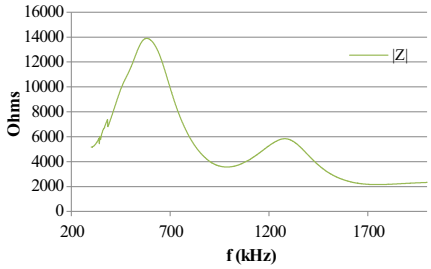

Figure 7. Coal and rock impedance between two bolts.

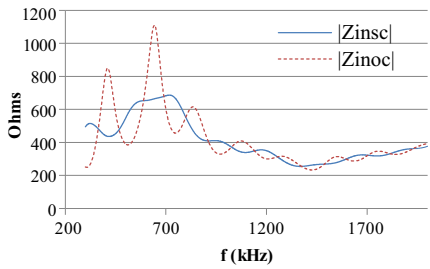

Figure 8. Open and shorted line impedance measurements of the single-conductor twisted cable.

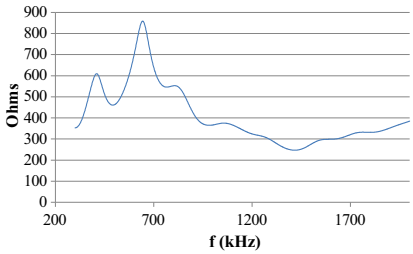

Figure 9. Characteristic impedance of the single-conductor twisted cable.

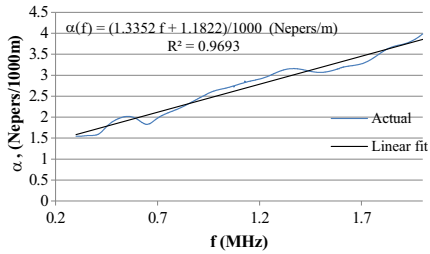

Figure 10. Attenuation constant of the single-conductor twisted cable.

4.4. Propagation Attenuation Constant

A propagation attenuation constant, $\alpha(f)$, of this single-conductor TL system is calculated from (6) using the measured results of the open and shorted TL. Figure 10 shows the attenuation constant as a function of frequency. The straight line shown in the figure is the linear least squares fit to the data. The linear equation given in the figure represents an empirical prediction of the attenuation constant of the TL in the SRCM environment.

4.5. Power Loss Rate

The power loss rate, $Loss(f)$, for the TL system is calculated from (5) and its frequency dependence is shown in Figure 11. The power loss rates are derived by multiplying the propagation attenuation constants 8.686. The power loss rate is in dB/length, but the attenuation is in Nepers/length, which is more connected to the analysis of a TL system. Similar to that of $\alpha(f)$, the power loss rate of the twisted cable TL system can be described by a linear equation. As shown in Figure 11, the power loss rate is low in the measured frequency band.

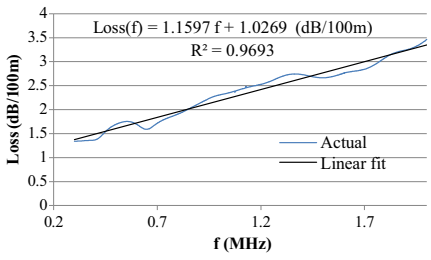

Figure 11. Power loss rate of the single-conductor twisted cable.

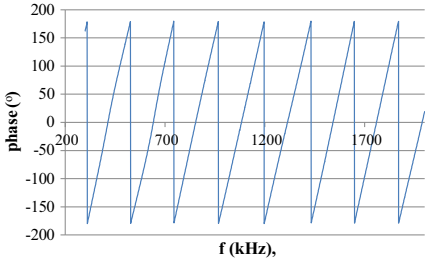

Figure 12. Input phase distribution, $2\beta(f)l$, of the single-conductor twisted cable.

4.6. Propagation Phase Constant

The phase constant as a function of frequency, $\beta(f)$, of the TL system was obtained from (7). Before using (7), the input phase distribution, $2\beta(f)l$, as a function of frequency needed to be obtained from (A20) where l is the length of the cable. After that, a number of pairs of frequencies, f_1 and f_2, were selected from the $2\beta(f)l$. Each pair of f_1 and f_2 was chosen such that $2\beta_2(f_2)l - 2\beta_1(f_1)l = \pm 2\pi$ radians. In this approach, the initial phase angle of $2\beta(f)l$ would not need to be known. Figure 12 shows the input phase distribution of the system, $2\beta(f)l$,

Table 1. Frequency pairs that result in exact 2π or 360° of their input phase angles.

f_1 (Hz)	f_2 (Hz)
310885	527711
527711	744110
744110	967578
967578	1196817
1196817	1431116
1431116	1648287
1648287	1869348

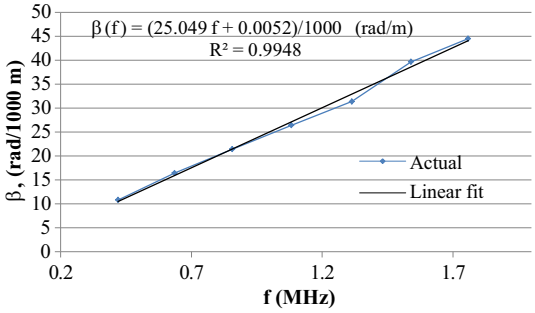

Figure 13. Phase constant of the single-conductor twisted cable.

obtained in this experiment. Many hundreds of pairs of frequencies could be candidates for selection from $2\beta(f)l$ covering the frequency range from 300 kHz to 2 MHz. With a TL system having a clearly linear distribution of its $2\beta(f)l$, only several pairs of frequencies were needed to estimate the $\beta(f)$ distribution. A group of seven pairs of f_2 and f_1 were selected in this experiment and are shown in Table 1. Figure 13 shows the resulting distribution of $\beta(f)$. As seen in the figure, the linear least squares fit line matched the calculated phase constant values very well, which is attributed to the good linearity of the input phase distribution.

Similar to that of other typical TL systems such as coaxial cables, the twisted cable configured as a single conductor showed a periodic characteristic and good linearity on its input phase distribution despite the nonlinear distribution of the coal and rock impedance in the tunnel. A single identifiable period and the linear input phase distribution are often essential to obtain a relatively accurate phase constant

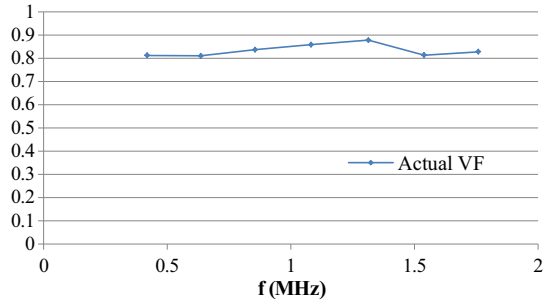

Figure 14. Velocity factor, $VF(f)$, of MF signals on the single-conductor twisted cable.

distribution, $\beta(f)$, for a TL system.

It should be noted that an input phase distribution with poor linearity or without a single identifiable period could signify that the measurements were corrupted often by a signal or signals comparable to the exciting signal, which might represent different propagation modes present on the TL system. Although the open and shorted line impedance measurements, $Z_{\text{inoc}}(f)$ and $Z_{\text{insc}}(f)$, have a periodic feature, that is not sufficient to guarantee a good linear input phase distribution with a single identifiable period. RF signals in different modes also present themselves as periodic signals on a TL system, possibly confounding the desired features. This could, indeed, be one way to distinguish good quality measurements from poor quality.

4.7. Velocity Factor of MF Signal

The velocity and the velocity factor, $VF(f)$, of the MF signals on the twisted cable TL system were determined from (8) and (9). The variation of the $VF(f)$ with frequency is given in Figure 14. The average $VF(f)$ was 0.834, which is coincidentally similar to some coaxial cables [15]. The nearly frequency independent $VF(f)$ distribution with a small standard deviation of 0.024 was attributed to the good linearity of $2\beta(f)l$. Similarly, our measurements also showed that coaxial cables have a near constant $VF(f)$ in MF band.

4.8. Discussions

Our measurements of a TL system composed of a conductor in a lossy coal mine tunnel demonstrate the importance of the electrical properties of coal and rock. Contrary to some other typical TL systems such as a coaxial cable, which is expected to have a constant

characteristic impedance over a wide frequency band, the single-conductor cable in the tunnel has a frequency-dependent characteristic impedance even over the narrow MF band as shown in Figure 9. This suggests that the frequency-dependent coal and rock impedances play a role in the cable's characteristic impedance. A similar result was reported in [6, 7].

The propagation phase constant and velocity factor obtained in the experiment do not show a high degree of sensitivity to the variation of the nonlinear coal and rock impedance distribution.

The impedances of the coal and rock in a tunnel had been reported to change over time, and in one case decreased by about 20% in 45 days, resulting in the power loss rate rising by 24%, and a considerably lower characteristic impedance in the same period in the frequency band from 200 kHz to 2 MHz [6, 7]. The TL propagation characteristic changes with time are likely due to the effects of humidity and temperature on the electrical properties of coal and rock. The method introduced in this paper offers a powerful tool for investigation of the changes of the propagation parameters in time.

In addition, the method can be used for a study of the influence of other factors on the propagation characteristics of MF signals on the TL system, such as positions of the TL in the tunnel, a tunnel with different dimensions or shapes, and temperature and moisture in the tunnel.

5. SUMMARY

We have presented a method to obtain the MF propagation characteristics of a long TL in a coal mine tunnel. The method requires measurements of the open and shorted TL impedances as a function of frequency, and yields the propagation parameters of the characteristic impedance, attenuation constant, phase constant, power loss rate, and velocity factor. Those parameters are needed to analyze and understand the performance of an MF communication system in a coal mine, which generally have a TL as its longest signal path. We presented measurement results of the MF propagation parameters on a single-conductor twisted pair cable TL system in a coal mine. We confirmed the low power loss of MF signals on the system. The experiment also showed that the coal walls and rock ceiling/floor in the tunnel had nonlinear impedance distributions which affected some of the MF propagation parameters. The method offers a general tool for obtaining the propagation characteristics of a TL system in a coal mine tunnel in support of an underground coal mine MF communication study.

6. DISCLAIMER

The findings and conclusions in this report are those of authors and do not necessarily represent the views of the National Institute for Occupational Safety and Health (NIOSH). The mention of any company or product does not constitute an endorsement by NIOSH.

ACKNOWLEDGMENT

The authors wish to thank Mr. Nicholas Damiano, Electrical Engineer, and Justin Srednicki, Electronics Technician, both of NIOSH for their assistance in experiment preparation and measurement data collection at SRCM. The authors wish also to thank Mr. Paul Stefko, the foreman of SRCM, for always facilitating and assisting our experimental work in SRCM.

APPENDIX A.

The formulas (1)–(9) are the basis of the method for determining the propagation parameters of a TL system, and can be found in many textbooks and publications including [9–14]. However, the complete derivation of these formulas can seldom be found within a single reference. For completeness, we present the deviation here with a unified notation. The derivation process also provides the procedure for obtaining the complex intermediate results from the primary measurements.

For the TL system shown in Figure 3 with a resistance per-unit-length, $R(f)$, inductance per-unit-length, $L(f)$, admittance per-unit-length, $G(f)$, and capacitance per-unit-length, $C(f)$, the Equations (A1) and (A2) govern the distributions of voltage, $V(f, x)$, and current, $I(f, x)$, along the line of a length x for a harmonic signal source with angular frequency $\omega = 2\pi f$.

$$\frac{dV(f,x)}{dx} = -[R(f) + j\omega L(f)]\, I(f,x) \tag{A1}$$

$$\frac{dI(f,x)}{dx} = -[G(f) + j\omega C(f)]\, V(f,x) \tag{A2}$$

Taking a derivative on both sides of (A1) and (A2) and inserting (A1) and (A2) into the resulting expressions, we obtain:

$$\frac{d^2V(f,x)}{dx^2} = [R(f) + j\omega L(f)]\,[G(f) + j\omega C(f)]\, V(f,x) = \gamma^2 V(f,x)$$

$$\frac{d^2I(f,x)}{dx^2} = [R(f) + j\omega L(f)]\,[G(f) + j\omega C(f)]\, I(f,x) = \gamma^2 I(f,x)$$

which can be rewritten as

$$\frac{d^2V(f,x)}{dx^2} - \gamma^2(f)\,V(f,x) = 0 \tag{A3}$$

$$\frac{d^2I(f,x)}{dx^2} - \gamma^2(f)\,I(f,x) = 0 \tag{A4}$$

These are two wave equations defined by a propagation constant, $\gamma(f)$, which can be determined by the per-unit-length electrical parameters of the TL as shown in (A5). $\gamma(f)$ has two components: the real component called the attenuation constant, $\alpha(f)$, and the imaginary component called the phase constant, $\beta(f)$, as given in (A5).

$$\gamma(f) = \sqrt{(R(f) + j\omega L(f))(G(f) + j\omega C(f))} = \alpha(f) + j\beta(f) \tag{A5}$$

The nonlinear relationship between the electrical parameters of the TL system and the propagation constant is clear from (A5), indicating that different electrical parameters of a TL can yield different propagation behaviors. Changes of these parameters, which can happen for a TL in different tunnels, will inevitably result in a value change of $\gamma(f)$.

Equations (A6) and (A7) are the general solutions of (A3) and (A4) in the steady state for both the voltage and current.

$$V(f,x) = V_0^+ e^{-\gamma(f)x} + V_0^- e^{\gamma(f)x} \tag{A6}$$

$$I(f,x) = I_0^+ e^{-\gamma(f)x} + I_0^- e^{\gamma(f)x} \tag{A7}$$

where V_0^+ and I_0^+ are forward incident voltage and current, and V_0^- and I_0^- are backward reflected voltage and current.

The current $I(f, x)$ can also be obtained from (A1) and (A6) as shown below.

$$\begin{aligned} I(f,x) &= \frac{\gamma(f)}{R(f) + j\omega L(f)} \left(V_0^+ e^{-\gamma(f)x} - V_0^- e^{\gamma(f)x}\right) \\ &= \frac{1}{Z_0(f)} \left(V_0^+ e^{-\gamma(f)x} - V_0^- e^{\gamma(f)x}\right) \end{aligned}$$

The complex quantity of $Z_0(f)$ is the characteristic impedance of the TL system. $Z_0(f)$ can be determined from (A8). Any change of its parameters can result in a change of a $Z_0(f)$.

$$Z_0(f) = \sqrt{\frac{R(f) + j\omega L(f)}{G(f) + j\omega C(f)}} \tag{A8}$$

If values of $R(f)$, $L(f)$, $G(f)$, and $C(f)$ are known, Equation (A8) can be conveniently used to determine the characteristic impedance of

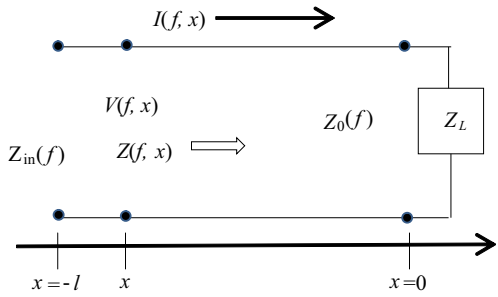

Figure A1. Impedance at a point of $x = -l$ along a terminated transmission line.

a TL system and (A5) can be used to determine the line's propagation constant. It is, however, not practical to measure $R(f)$, $L(f)$, $G(f)$ and $C(f)$ in a mine environment, especially over distances of kilometers.

It is known that for a TL terminated with a load Z_L as shown in Figure A1, there will be a reflected wave for voltage and current, and the reflection coefficient can be determined using (A9) [13]. With the reference point set at the load side ($x = 0$) on the line, the impedance at any point in a distance of x from the reference point can be determined by (A10). At the input terminal of $x = -l$, the input impedance $Z_{\text{in}}(f)$ can then be determined by (A11). The open circuit impedance, $Z_{\text{inoc}}(f)$ with $Z_L = \infty$, can be obtained from (A12) and the short circuit impedance, $Z_{\text{insc}}(f)$ with $Z_L = 0$, from (A13) of the TL. Multiplying both sides of (A12) and (A13), we can obtain (A14) the characteristic impedance, $Z_0(f)$, of the TL.

$$\Gamma(f) = \frac{Z_L - Z_0(f)}{Z_L + Z_0(f)} \tag{A9}$$

$$\begin{aligned} Z(f,x) &= \frac{V(f,x)}{I(f,x)} = \frac{V_0^+\left(e^{-\gamma(f)x} + \Gamma(f)e^{\gamma(f)x}\right)}{\frac{V_0^+}{Z_0(f)}\left(e^{-\gamma(f)x} - \Gamma(f)e^{\gamma(f)x}\right)} \\ &= Z_0(f)\frac{Z_L - Z_0(f)\tanh(\gamma(f)x)}{Z_0(f) - Z_L\tanh(\gamma(f)x)} \end{aligned} \tag{A10}$$

$$Z_{\text{in}}(f) = Z(f, x = -l) = Z_0(f)\frac{Z_L + Z_0(f)\tanh(\gamma(f)l)}{Z_0(f) + Z_L\tanh(\gamma(f)l)} \tag{A11}$$

$$Z_{\text{inoc}}(f) = Z_0(f)\frac{\infty + Z_0(f)\tanh(\gamma(f)l)}{Z_0(f) + \infty\tanh(\gamma(f)l)} = Z_0(f)\coth(\gamma(f)l) \tag{A12}$$

$$Z_{\text{insc}}(f) = Z_0(f)\frac{0 + Z_0(f)\tanh(\gamma(f)l)}{Z_0(f) + 0\tanh(\gamma(f)l)} = Z_0(f)\tanh(\gamma(f)l) \quad \text{(A13)}$$

$$Z_0(f) = \sqrt{\frac{Z_{\text{inoc}}(f)}{\coth(\gamma(f)l)} \cdot \frac{Z_{\text{insc}}(f)}{\tanh(\gamma(f)l)}} = \sqrt{Z_{\text{inoc}}(f)Z_{\text{insc}}(f)} \quad \text{(A14)}$$

Expression (A15) can also be obtained from (A12) and (A13), the result is assumed to be a complex quantity A. Expression (A16) can be obtained from (A15) with $\gamma(f) = \alpha(f) + j\beta(f)$. The real part of (A16) is given in (A17). The attenuation constant, $\alpha(f)$, can then be solved with (A18). Similarly, the power loss rate can be solved using (A19). From (A16), the input phase, $2\beta(f)l$, can also be obtained and is given in (A20) where φ is the initial phase angle. Because of the periodic nature of the signal, the input phase values repeat every $\pm 2\pi$. Selecting $2\beta_1(f_1)l$ at f_1 and $2\beta_2(f_2)l$ at f_2 such that $2\beta_2(f_2)l$ and $2\beta_1(f_1)l$ have an exact difference of 2π radians as shown in (A21) to eliminate the initial phase for phase constant calculation, yields (A22).

$$\sqrt{\frac{Z_{\text{insc}}(f)}{Z_{\text{inoc}}(f)}} = \sqrt{\frac{Z_0(f)\tanh(\gamma(f)l)}{Z_0(f)\coth(\gamma(f)l)}} = \tanh(\gamma(f)l)$$

$$= \frac{e^{2\gamma(f)l} - 1}{e^{2\gamma(f)l} + 1} = A(f) \quad \text{(A15)}$$

$$e^{2\gamma(f)l} = \frac{1 + A(f)}{1 - A(f)} = \text{Re}(f)e^{j\theta(f)} = e^{2(\alpha(f) + j\beta(f))l} = e^{2\alpha(f)l}e^{j2\beta(f)l} \quad \text{(A16)}$$

$$e^{2\alpha(f)l} = \text{Re}(f) = \left|\frac{1 + A(f)}{1 - A(f)}\right| \quad \text{(A17)}$$

$$\alpha(f) = \frac{1}{2l}\ln\left|\frac{1 + A(f)}{1 - A(f)}\right| = \frac{1}{2l}\ln\left|\frac{1 + \sqrt{\frac{Z_{\text{insc}}(f)}{Z_{\text{inoc}}(f)}}}{1 - \sqrt{\frac{Z_{\text{insc}}(f)}{Z_{\text{inoc}}(f)}}}\right| \left(\frac{\text{Nepers}}{\text{Unit length}}\right) \quad \text{(A18)}$$

$$\text{Loss}(f) = 20\log e^{\alpha(f)\cdot 1} = \frac{8.686}{2l}\ln\left|\frac{1 + \sqrt{\frac{Z_{\text{insc}}(f)}{Z_{\text{inoc}}(f)}}}{1 - \sqrt{\frac{Z_{\text{insc}}(f)}{Z_{\text{inoc}}(f)}}}\right| \left(\frac{\text{dB}}{\text{Unit length}}\right) \quad \text{(A19)}$$

$$2\beta(f)l = \theta(f) = \arctan\left(\frac{\text{im}\left(\frac{1 + A(f)}{1 - A(f)}\right)}{\text{real}\left(\frac{1 + A(f)}{1 - A(f)}\right)}\right) + \varphi + 2n\pi,$$

$$n = 0, \pm 1, \pm 2, \ldots \quad \text{(A20)}$$

$$2\beta_2(f_2)l - 2\beta_1(f_1)l = 2\pi \quad \text{(A21)}$$

$$\beta_2(f_2) - \beta_1(f_1) = \frac{\pi}{l} \quad \text{(A22)}$$

The wave propagation velocity can be determined with (A23). The phase constant equation can then be written in (A24). Substituting (A24) into (A22), we obtain (A25). Consequently, the velocity can be obtained from (A26) with an assumption of an equal velocity for all frequencies. The velocity factor can be solved with (A27), where the velocity of light is 3.0×10^8 m/s. Substituting (A25) into (A24) and letting $f = (f_2 + f_1)/2$, the value of phase constant can then be obtained and is given in (A28).

$$v_p(f) = \frac{\omega}{\beta(f)} = \frac{2\pi f}{\beta(f)} \tag{A23}$$

$$\beta(f) = \frac{2\pi f}{v_p} \tag{A24}$$

$$\frac{2\pi f_2}{v_p(f_2)} - \frac{2\pi f_1}{v_p(f_1)} = \frac{\pi}{l} \tag{A25}$$

$$v_p\left(f = \frac{f_2 + f_1}{2}\right) = 2l(f_2 - f_1)(m), \quad f_1 \text{ and } f_2 \text{ in Hz} \tag{A26}$$

$$VF(f) = \frac{v_p}{3.0 \times 10^8} \tag{A27}$$

$$\beta\left(f = \frac{f_2 + f_1}{2}\right) = \frac{2\pi f}{v_p} = \frac{2\pi(f_2 + f_1)/2}{2x(f_2 - f_1)}$$
$$= \frac{\pi(f_2 + f_1)}{2l(f_2 - f_1)} \quad \left(\frac{\text{rad}}{\text{unit length}}\right) \tag{A28}$$

REFERENCES

1. Stolarczyk, L. G., "Emergency and operational low and medium frequency band communications system for underground mines," *IEEE Transactions on Industry Applications*, Vol. 27, No. 4, 780–790, Jul./Aug. 1991.
2. Stolarczyk, L. G. and H. Dobroski, "Medium frequency vehicular control and communication systems for underground mines," *IEEE Vehicular Technology Conference*, 316–321, May 21–23, 1984.
3. Dobroski, H. and L. G. Stolarczyk, "Control and monitoring via medium-frequency techniques and existing mine conductors," *IEEE Transactions on Industry Applications*, Vol. 21, No. 4, 1087–1092, Jul. 1985.
4. Stolarczyk, L. G., "A medium frequency wireless communication system for underground mines," 83–103, A.R.F. Products, Inc.,

Raton, New Mexico, A Mining Contract Research Report, Contract HO308004, Sep. 20–22, 1984.

5. Stolarczk, L. G., M. Sepich, and K. Smoker, "A medium frequency wireless communication system for underground mines," Report from A.R.F. Products, Inc., Raton, New Mexico, 87740 to Bureau of Mines, Jan. 1983.
6. Li, J., B. Whisner, and J. Waynert, "Measurements of medium frequency propagation characteristics of a transmission line in an underground coal mine," *Record of IEEE IAS Annual Meeting*, 1–8, Las Vegas, NV, USA, 2012-MIC-343, Oct. 7–11, 2012.
7. Li, J., B. Whisner, and J. Waynert, "Measurements of medium frequency propagation characteristics of a transmission line in an underground coal mine," *IEEE Trans. on IAS*, Vol. 49, No. 5, 1–8, Sep./Oct. 2013.
8. Carson, J. R., "Wave propagation in overhead wires with ground return," *Bell System Technical Journal*, Vol. 5, 539–553, 1926.
9. D'Amore, M. and M. Sabrina, "Simulation model of a dissipative transmission line above a lossy ground for a wide-frequency range — Part I: Single conductor configuration," *IEEE Transactions on Electromagnetic Compatibility*, Vol. 38, No. 2, 127–138, May 1996.
10. Degauque, P., G. Courbet, and M. Heddebaut, "Propagation along a line parallel to the ground surface: Comparison between the exact solution and the quasi-TEM approximation," *IEEE Transactions on Electromagnetic Compatibility*, Vol. 25, No. 4. 422–427, Nov. 1983.
11. Agrawal, A., K. Lee, L. Scott, and H. Fowles, "Experimental characterization of multiconductor transmission lines in the frequency domain," *IEEE Transactions on Electromagnetic Compatibility*, Vol. 21, No. 1, 20–27, Feb. 1997.
12. Volakis, J., *Antenna Engineering Handbook*, 4th Edition, 51-3–51-43, 2007.
13. Shevgaonkar, G. R. K., "Transmission lines and EM waves," Online Lecture Series, Department of Electrical Engineering, IIT, Bombay, Jan. 8, 2008.
14. Paul, C. R., *Analysis of Multiconductor Transmission Lines*, 2nd Edition, 240–278, Published by A John Wiley & Sons, Inc., 2007.
15. *Coaxial Cable*, http://en.wikipedia.org/wiki/Coaxial_cable.